Revision 1

Quasicrystals at extreme conditions: The role of pressure in stabilizing icosahedral $Al_{63}Cu_{24}Fe_{13}$ at high temperature

VINCENZO STAGNO[1, 2, 3*], LUCA BINDI[4], CHANGYONG PARK[5], SERGEY TKACHEV[6], VITALI B. PRAKAPENKA[6], H.-K. MAO[1,7], RUSSELL J. HEMLEY[1], PAUL J. STEINHARDT[8], YINGWEI FEI[1]

[1]Geophysical Laboratory, Carnegie Institution of Washington, Washington, DC 20015, USA.

[2]Geodynamics Research Center, Ehime University, Matsuyama, Japan.

[3] Earth-Life Science Institute, Tokyo Institute of Technology, Tokyo 152-8550, Japan

[4]Dipartimento di Scienze della Terra, Università di Firenze, Via La Pira 4, I-50121 Florence, Italy.

[5]HPCAT, Geophysical Laboratory, Carnegie Institution of Washington, Argonne, IL 60439, USA

[6]Center for Advanced Radiation Sources, University of Chicago, Chicago, Illinois 60637, U.S.A.

[7]Center for High Pressure Science and Technology Advanced Research, Shanghai 201203, P. R. China.

[8] Department of Physics and Princeton Center for Theoretical Science, Princeton University, Princeton, New Jersey 08544, USA.

*Corresponding author: Vincenzo Stagno, Geodynamics Research Center, Ehime University, Matsuyama, Japan. Email: vin.stagno@elsi.jp

Abstract

Icosahedrite, the first natural quasicrystal with composition $Al_{63}Cu_{24}Fe_{13}$, was discovered in several grains of the Khatyrka meteorite, a CV3 carbonaceous chondrite. The presence of icosahedrite associated with high-pressure phases like ahrensite and stishovite indicates formation at high pressures and temperatures due to an impact-induced shock. Previous experimental studies on the stability of synthetic icosahedral AlCuFe have either been limited to ambient pressure, for which they indicate incongruent melting at ~1123 K, or limited to room temperature, for which they indicate structural stability up to about 35 GPa. These data are insufficient to experimentally constrain the formation and stability of icosahedrite under the conditions of high pressure and temperature that formed the Khatyrka meteorite. Here we present the results of room-temperature, high pressure diamond anvil cells measurements of the compressional behavior of synthetic icosahedrite up to ~50 GPa. High *P-T* experiments were also carried out using both laser-heated diamond anvil cells combined with in situ synchrotron X-ray diffraction (at ~42 GPa) and multi-anvil apparatus (at 21 GPa) to investigate the structural evolution and crystallization of possible coexisting phases. The results demonstrate that the quasiperiodic order of icosahedrite is retained over the *P-T* range explored. We find that pressure acts to stabilize the icosahedral symmetry at temperatures much higher than previously reported. Direct solidification of AlCuFe quasicrystals from an unusual Al-Cu-rich melt is possible but it is limited to a narrow temperature range. Alternatively, quasicrystals may form after crystallization through solid-solid reactions of Al-rich phases. In either case, our results show that quasicrystals can preserve their structure even after hypervelocity impacts spanning a broad range of pressures and temperatures.

Keywords: Icosahedrite, Quasicrystals, CV3 chondrite, redox, Khatyrka meteorite, solar nebula.

Introduction

Quasicrystals (QC; Levine and Steinhardt 1984; Shechtman et al. 1984) represent a class of solids characterized by quasiperiodic translational order and crystallographically-forbidden rotational symmetries and are now observed in nature (Bindi et al. 2009). These symmetries include the icosahedral (i) symmetry exhibited by $Al_xCu_yFe_z$ alloys, where x varies between 61 and 64, y is 24-26 and z 12-13 atomic% (Bancel 1999). This chemical interval corresponds to the compositional range at which the i-QC solely is stable up to ~1023 K at ambient pressure. Above this temperature the stability field of the quasicrystal decreases to a very narrow chemical composition up to ~1123 K, where the i-QC with composition $Al_{62.5}Cu_{25}Fe_{12.5}$ coexists with a liquid + (λ) monoclinic phase with composition $Al_{13}Fe_4$ (Tsai 2013; Zhan and Lück 2003a-e). At temperatures above ~1200 K, i-QC has been shown to be unstable, such that the liquid only coexists with the λ phase. At approximately 1300 K the system is totally molten and the liquid composition reflects that of the starting QC.

Experimental studies of the phase relationships at ambient pressure have been the only available tool to date to constrain the origin of the first natural quasicrystal, icosahedrite $Al_{63}Cu_{24}Fe_{13}$ (Bindi et al. 2009, 2011). However, textural and petrographic evidence suggest that the natural quasicrystal formed in outer space under pressures and temperatures considerably higher than 1 bar and 1300 K (Bindi et al. 2012; Hollister et al. 2014). Recently, Stagno et al. (2014) performed *in situ* high *P*-*T* X-ray diffraction studies and showed that the icosahedral symmetry of the AlCuFe QC is retained at 5 GPa and temperatures up to 1673 K. Above this temperature the synthetic icosahedrite used for the experiments was found to decompose to a liquid in equilibrium with CuAl (corresponding to the mineral cupalite, an accessory phase also found in the Khatyrka meteorite), and the cubic β phase (Bindi et al. 2011). Although this study

provided information on the compressional behavior of i-AlCuFe QC, the results gave only a lower-bound on the *P-T* stability of natural icosahedrite. Previous studies that focused on the compressional behavior and structural stability of QCs with compositions slightly different from that of icosahedrite include measurements on i-$Al_{62}Cu_{25.5}Fe_{12.5}$, which was shown to be stable up to 35 GPa (Sadoc et al. 1994, 1995; Lefebvre et al. 1995).

Here we present experimental results using both diamond anvil cell (DAC) and multi-anvil techniques to investigate the stability of synthetic i-AlCuFe at higher pressures and temperatures than those reported in previous studies. We show that the icosahedral structure is stabilized at high temperature as pressure increases, which makes quasicrystal behavior similar to that of most crystalline materials exposed to similar extreme conditions. Our results indicate that icosahedrite could have formed within a large range of pressures and temperatures during the formation of our solar system provided extremely reducing conditions. Hence, Khatyrka might represent one of many QC-bearing meteorites in our solar system or elsewhere in the cosmos.

Experimental Methods

The synthetic icosahedral quasicrystal used as starting material was characterized by SEM and XRD measurements and shown to have the formula $Al_{63}Cu_{24}Fe_{13}$ (Bancel 1999) plus minor amounts of cupalite, (Cu,Fe)Al. The synthetic material was first broken in several small fragments. A small chip was, then, loaded in a diamond anvil cell with culet size of 600 μm and crushed to a fine powder by hand loading. A small portion of the powder with dimensions of about 30 × 30 μm was picked with a needle and placed at the center of a symmetric diamond anvil cell with 300 μm culet size using a Re gasket as sample chamber with a 150 μm diameter

hole. A couple of ruby spheres were placed next to the sample as pressure markers. One diamond anvil was supported by a cubic boron nitride (c-BN) backing plate, and the other anvil by a tungsten carbide (WC) backing plate. *In situ* angle-dispersive powder X-ray diffraction measurements were performed at high pressure at the 16BM-D beamline, HPCAT (Advanced Photon Source, APS, Argonne National Laboratory, ANL). The DAC was loaded with Ne, which served as both a pressure medium and a pressure marker (Hemley et al. 1989), and then mounted on a motor driven gearbox with the WC seat on the downstream side, and the c-BN seat on the upstream side. Sample pressures were measured with the ruby luminescence method (Mao et al. 1986) through an on-line system. Monochromatic incident X-ray beams with wavelengths of 0.42460 Å and 0.5166 Å were used. The beam was focused to a spot of 5 × 15 μm by using a pair of Kirkpatrick-Baez mirrors. The MAR345 image plate detector was placed at a distance approximately 478 mm from the sample in order to obtain high resolution and accuracy of the Debye-Scherrer diffraction rings. Diffraction peaks were collected using a continuous ω-oscillation scan mode over the range from -6° to +6° with an exposure time of 180 seconds.

Simultaneous high-pressure and temperature synchrotron powder X-ray diffraction experiments were conducted at the 13ID-D beamline, GSECARS (APS, ANL) using a focused monochromatic 30 keV X-ray beam with wavelength 0.4133 Å. Double-sided laser heating was performed using two infrared laser beams focused to 15 μm flat-top spots on both sides of the sample co-axially aligned with two optical paths for temperature measurements and visually aligned with focused 4 μm X-ray beam using the X-ray induced luminescence of the sample (Prakapenka et al. 2008). Laser power was adjusted independently on upstream and downstream sides to control the sample temperature within ±100K. The target temperature was maintained for about 10 min. Temperatures of the laser-heated sample were measured using thermal

radiation spectra fitted to the blackbody radiation function. Diffraction patterns were collected on a MarCCD-165 detector with exposure time of 15 s. In these experiments, chips of synthetic $Al_{63}Cu_{24}Fe_{13}$ were also crushed and then slightly pressed to form a platelet. A small platelet with a diameter of approximately 60 μm was loaded into the sample chamber of a symmetric diamond-anvil cell with flat anvils of 300 μm-size culet. Pressure was measured using the thermal equation of state of Ne used as pressure medium. The *in situ* X-ray diffraction patterns were processed using FIT2D software (Hammersley 1998), and the *d*-spacing relative to each reflection was determined using PeakFit software.

Quench experiments were performed at 21 GPa and temperature between 1600 K and 2000 K using a 1500-ton Walker-type press available at the Carnegie Institution of Washington. The starting material used in this study was a synthetic icosahedral AlCuFe (≥99.9%) quasicrystalline powder with nominal composition of $Al_{65}Cu_{23}Fe_{12}$, according to a previous study (Stagno et al. 2014). Tungsten carbide anvils of 3 mm truncation edge length (TEL) were used with 8 mm edge length MgO pressure media. Graphite and alumina capsules were used in the attempt to prevent oxidation of the starting material. The capsules were then placed in the central portion of a cylindrical Re furnace, surrounded by MgO sleeve and spacers. A $LaCrO_3$ sleeve was used as thermal insulator outside the heater.

Details of the pressure calibration of this type of assembly have been reported by Hirose and Fei (2002). The temperature during the experiment at 1973 K was monitored with a W-5%Re/W-26%Re (C-type) thermocouple inserted within an alumina sleeve, with the junction in contact with the top of the capsule. From this run, a temperature versus power calibration curve was obtained that was used for the additional runs. The sample was compressed to the target pressure at a rate of 0.5 GPa/hr, and then heated to the target temperature and kept manually

constant within 10 K for a period of 15-60 minutes. The sample was quenched by turning off the power to the furnace and, then, decompressed to ambient pressure.

All recovered samples from quench experiments were mounted in epoxy resin and polished parallel to the axial furnace direction for textural observation and chemical composition mapping by Field Emission Scanning Electron Microscope (JEOL JSM 6500F). Semi-quantitative analyses using energy-dispersive X-ray spectroscopy, were performed at 15 kV and 1.1 nA using metals (Fe, Cu, Al,) and oxides (Al_2O_3) as standards. Phase identification of the selected recovered run products was accomplished using an Oxford Diffraction Xcalibur PX Ultra single-crystal diffractometer fitted with a 165 mm diagonal Onyx CCD detector (Cu*K*α radiation). The crystal-to-detector distance was 7 cm. Data were processed using the *CrysAlis* software package version 1.171.31.2 (Oxford diffraction) running on the Xcalibur PX control PC.

Results and Discussion

Compression behavior

Synthetic icosahedral quasicrystals with the formula $Al_{63}Cu_{24}Fe_{13}$ (Bancel 1999) were used as starting materials for our *in situ* DAC experiments. An accurate textural and chemical analyses of the synthetic material showed minor amounts of (Cu, Fe)Al. The first set of experiments consisted of *in situ* powder angle-dispersive X-ray diffraction measurements on i-QC using DACs up to ~50 GPa at room temperature. These experiments aimed to investigate the evolution of the icosahedral structure under pressure, the determination of the lattice parameter and the equation of state. A total of 50 diffraction patterns were collected during compression

158 and decompression. Figure 1 shows a characteristic spotty diffraction pattern constantly observed
159 during our experiments and resulting from heterogeneous size of the QC grains.

160 Figure 2 shows the variation of the *d*-spacing for 7 known diffraction peaks with
161 increasing pressure and after decompressing the sample to ambient pressure. The intensities of
162 the peaks appear strongly affected by the preferred orientation of the powder grains as can be
163 observed in Figure 1. The shift in *d*-spacing with increasing pressure can also be seen for most of
164 the peaks up to the target pressure. In addition, the peak broadening is apparent as the pressure
165 increases and can be attributed to an increase of the mosaic spread and local strains. After the
166 sample was decompressed to ambient pressure, peaks were still broadened in agreement with
167 what was reported by Sadoc et al. (1994) for i-$Al_{62}Cu_{25.5}Fe_{12.5}$.

168 We collected additional diffraction patterns at higher resolution by moving the detector to
169 a farther distance from the sample (~478 mm). This allowed us to investigate more accurately the
170 icosahedral structure, in particular the behavior in the high *d*-spacing region that included peaks
171 (12,16) at 5.53 Å and (8,4) at 8.94 Å, respectively [for indexing notation see Lu et al. (2001)].
172 Diffraction patterns collected up to 36 GPa clearly show a gradual broadening with increasing
173 pressure (Figure S1). Two additional peaks belonging to i-AlCuFe were also observed with *d*-
174 spacings of ~6 Å and 9.7 Å that could be indexed as (24,15) and (6,3), respectively, using the
175 automated identification scheme described by Lu et al. (2001), or may be reflections due to
176 a minor unidentified phase. Our *in situ* X-ray diffraction measurements show that no peaks
177 appear or disappear up to the target pressure of ~50 GPa, which excludes possible pressure-
178 induced phase transformations, including amorphization, that has been found to occur for i-
179 AlLiCu quasicrystals (Itie et al. 1996). The observed peak broadening with pressure can be

interpreted as arising from the increasing atomic disorder, perhaps due to residual stress, without changing the long-range quasicrystalline order.

We determined the pressure dependence of the lattice parameter a_{6D} up to the maximum pressure of ~50 GPa (see Table S1 of Supporting Information). The parameter is defined as,

$$a_{6D} = d\sqrt{\frac{N+M\tau}{2(2+\tau)}} \quad (1),$$

where d is the d-spacing in Å, N and M the Cahn indices for which the d-spacing is experimentally determined, and τ is the golden ratio, (1+√5)/2 (Steurer and Deloudi 2009). The six-dimensional lattice parameter is shown to gradually decrease with increasing pressure (Fig. 3). The slightly scattered data at 24-32 GPa is likely due to the less accurate pressure determination caused by the overlap between the (111) peak of Ne and the (80, 128) peak of i-AlCuFe. However, the lattice parameter calculated from compression experiments is in good agreement with that calculated on decompression. The estimated reduction of the lattice parameter from the ambient pressure value of 12.64 Å is about 8%. In addition, our a_{6D} value at 5 GPa and room temperature is consistent with that determined by Stagno et al. (2014) at similar conditions. We conclude that the QC retains its icosahedral structure over the pressure range investigated. Further studies are needed to distinguish whether the stability is thermodynamic or kinetic.

The zero pressure bulk modulus K_0 and its pressure derivative K_0' were determined from the least-squares fit to several equation of state (EOS) models. Fit to the first-order Murnaghan EOS fit (Angel et al. 2014), which allows direct comparison with the results of previous studies, resulted in K_0 = 113.7(±2.9) and K_0' = 4.22(±0.22). It can be seen from Figure 4 that K_0 and K_0'

obtained from our data are significantly lower and higher, respectively, than those obtained for $Al_{62}Cu_{25.5}Fe_{12.5}$ from previous authors using the same EOS, i.e., K_0 = 139(±6) GPa and K_0' = 2.7 (Sadoc et al. 1994), and K_0 = 155(±10) GPa and K_0' = 2 (Lefebvre et al. 1995). Our EOS parameters also differ from those determined for an approximant phase with composition $Al_{64}Cu_{24}Fe_{12}$ that is close to our synthetic i-QC [K_0 = 175(±16) GPa and K_0' = 2.00 (Lefebvre et al. 1995)]. Such differences in the compressional behavior can be interpreted as due to either different composition of the QCs or distinct mechanical properties of the approximant (crystalline) phase. It should be kept in mind, however, that in previous studies in which DACs techniques were employed, silicon oil was used as a pressure medium, for which hydrostaticity is limited to very low pressure (Angel et al. 2007). Moreover, the previously suggested EOSs have been derived from data collected using energy-dispersive rather than angle-dispersive X-ray diffraction with the lattice parameter calculated using a different peak than the (8,4) used in this study without taking into consideration possible anisotropy of the material.

Our experimental data were also fit using both a third-order Birch-Murnaghan EOS [K_0 = 110.4(±2.9) and K_0'= 4.79(±0.28)] and a Vinet et al. EOS [K_0 = 109.4(±2.9) and K_0' = 5.06(±0.29)]. Whereas the resulting parameters deviate slightly from the parameters obtained using a simple Murnaghan model, they confirm the lower bulk modulus of synthetic icosahedrite compared to literature data. Figure 4 also shows the compressional behavior for pure *fcc*-Al, *fcc*-Cu (Dewaele et al. 2004) and *hcp*-Fe (Mao et al. 1990) plotted using the Vinet et al. and Birch-Murnaghan EOS models. For all these pure metals the structure has been reported to be stable over a wide pressure range > 100 GPa. As observed by Sadoc et al. (1994), the compressional behavior of our synthetic icosahedrite is much closer to that of pure Cu, although Al represents the main constituent. We therefore expect a similar compressional behavior for i-AlCuFe

226 quasicrystals varying in compositions according to the phase diagram proposed by Bancel
227 (1999).
228
229 High *P*-*T* stability of icosahedral symmetry

230 Recently, the conditions for the formation of natural i-AlCuFe have been constrained on
231 the basis of textural and chemical analyses of the coexisting mineral phases within the CV3-like
232 chondritic grains of the Khatyrka meteorite (Hollister et al. 2014; MacPherson et al. 2013). The
233 observation of rare Al-Cu-Fe alloys associated with melt droplets and phases such as stishovite
234 and ahrensite imply that the meteorite was subjected to a combination high pressures and
235 temperatures resulting from a high-velocity impact-induced shock. A study of icosahedrite at
236 high pressures and temperatures enables more definitive understanding of the petrological
237 processes that formed the Khatyrka meteorite. A first study by Stagno et al. (2014) indicated that
238 synthetic icosahedrite is stable at 5 GPa at temperatures up to ~1673 K; at higher temperatures,
239 the sample was found to melt incongruently and produce two solid crystalline phases: β-phase
240 and cupalite. These experiments provided the first indication that pressure might act to stabilize
241 the QC at *T* higher than 1300 K.

242 *In situ* high *P*-*T* laser heating system diamond-anvil cell experiments were conducted to
243 further constrain the stability field of icosahedrite. The synthetic quasicrystalline powder was
244 first compressed to ~42 GPa, then heated to ~ 1830 K while collecting X-ray diffraction patterns
245 to monitor any possible transformation or melting (see details in the Experimental Methods
246 session). The sample was then cooled down to 1000 K before being quenched. The results show
247 that during heating at about 1560 K the intensity of most of the peaks decreases dramatically,
248 and new peaks belonging to the QC phase appear at *d*-spacings between 1.8 and 2.0 Å (Fig. 5).

Interestingly, during cooling of the sample at about 1500 K the main peaks re-appear and are visible even after quenching the sample to room *T*. No amorphization or phase transformation was evident, and the new peaks that are characteristic of the QC become visible as a result of a strong preferential orientation. However, with increasing *T* the loss of quasicrystallinity (i.e., formation of crystal approximants) via a reversible process cannot be excluded.

Because of the small size of the laser spot, it is possible to heat different points of the sample within the DAC. The results of the high *T* run performed at the same pressure for a different point of the sample is shown in Fig. S2. In this case the QC was heated up to ~2110 K and then quenched directly to room temperature. The results are similar to the previous experiment at 1600 K, where peaks characteristic of synthetic icosahedrite were present. At higher *T*, new unknown peaks appear that are preserved also after quenching the sample to room temperature suggesting that the i-QC might have decomposed irreversibly. However, subsequent *ex situ* single crystal X-ray diffraction measurements on a micrometer-sized grain handpicked from the cell (see Fig. S3 of Supporting Information) showed that, at least for that fragment of the sample, the 5-fold symmetry characteristic of i-QC is retained. Given the difficulty to establish whether or not the *ex situ* fragment was heated all the way up to the target temperature, we cannot extend with confidence the ex-situ results to the bulk heated sample.

We performed additional quench experiments using the multi-anvil technique to better understand the nature of the unknown peaks discussed above. Experiments were performed at 21 GPa and temperatures between 1673 and 1993 K for icosahedral AlCuFe (≥99.9%) quasicrystalline powder with nominal composition of $Al_{65}Cu_{23}Fe_{12}$ previously characterized (Stagno et al. 2014). SEM images using back-scattered electrons of the run products reveal the compositions and textures of the recovered material (Fig. 6). The run quenched from 1673 K

consists of a single phase with composition $Al_{64.11(\pm0.66)}Cu_{24.70(\pm0.74)}Fe_{11.19(\pm0.22)}$, which is consistent with the starting composition of the synthetic QC. Several grains showed a patchy texture that we believe are due to the onset of melting of the QC. At about 1773 K the recovered sample shows the coexistence of β-phase ($Al_{64.73(\pm0.36)}Cu_{20.23(\pm0.91)}Fe_{15.04(\pm0.68)}$), Fe-rich cupalite ($Al_{48.77(\pm0.35)}Cu_{36.10(\pm0.93)}Fe_{15.13(\pm0.70)}$) and a phase identified by the patchy texture with composition $Al_{62.65(\pm0.89)}Cu_{33.52(\pm1.08)}Fe_{2.92(\pm0.27)}$ that can be interpreted either as a Fe-poor khatyrkite ($CuAl_2$) or a melt. Small grains of Al_2O_3 are also present and suggest possible oxidation of the material during the experiment. Finally, the recovered sample from 1973 K appears totally molten consisting of a Fe-rich liquid with composition $Al_{12.07(\pm0.50)}Cu_{21.34(\pm1.04)}Fe_{65.48(\pm0.73)}$ and exhibiting a characteristic quench texture that includes "skeletal" Al metal (Fig. 6d).

The results of quench experiments thus, suggest 1) that the QC retains its stability at 21 GPa and 1673 K and its icosahedral symmetry is retained after quench; 2) as temperature increases isobarically icosahedrite might melt congruently to, then, dissociate in a liquid with composition very similar to khatyrkite + β-phase + cupalite similar to what was reported by Stagno et al. (2014); 3) pure Al is the first phase crystallizing from a molten liquid with icosahedrite-like composition.

Implications

Our experimental results reproduce key features associated with the presence of icosahedrite that have been observed in the Khatyrka meteorite in terms of the phase assemblage (cupalite, β-phase, khatyrkite and pure Al) and texture. The coexistence of icosahedrite with a liquid phase having the same composition (i.e. congruent melting) than the ideal composition

295 reported by Bancel (1999; i.e., $Al_{63}Cu_{24}Fe_{13}$) has been never reported at such high pressures and
296 implies that the i-QC is kinetically stable and perhaps thermodynamically stable at high pressure.
297 This would confirm the hypothesis by Hollister et al. (2014) that the Al, Cu-rich assemblage in
298 the Khatyrka meteorite formed after an impact-induced shock followed by rapid cooling. (10^2-
299 10^3 °C s^{-1}) from which the Al, Cu-rich assemblage formed. However, we point out that a similar
300 mechanism of formation for icosahedrite appears unlikely as we assume here thermodynamic
301 equilibrium between the QC and the liquid from which it forms. In fact, the coexistence of Al,
302 Cu rich-phases with icosahedrite in the Khatyrka meteorite would suggest an initial high
303 abundance of these elements, as confirmed by the finding of Al-rich Cu-bearing FeNi and sulfide
304 phases in proximity of the QC. The finding of pure Al in our experiments is a further element of
305 similarity with the natural assemblage (see Fig. 2 in Hollister et al. 2014) and can be explained in
306 light of its lower melting temperature with respect to Fe and Cu that would trigger its
307 mobilization by diffusion mechanisms and exsolution. At 1773 K the presence of khatyrkite
308 coexisting with pure Al would represent a further evidence of the high-temperature regime
309 occurred during crystallization of these phases that would require an unusual abundance of Al.
310 To date, two hypotheses have been proposed (Hollister et al. 2014) to explain the origin
311 of Al-Cu-Fe alloys in the Khatyrka meteorite: 1) formation by an impact-induced shock event
312 that causes the diffusion of Al and Cu out of FeNi initially enriched with Al and Cu; or 2)
313 formation during nebular processes before the impact occurred and re-melting and re-
314 solidification of these alloys after the impact. In either case, the impact event enables
315 mechanisms such as diffusion, solid-solid reactions and oxidation-reduction. Although the
316 processes occurring in the meteorite cannot be precisely reproduced in laboratory experiments, it
317 is notable that our experiments lead to the same phases even at pressures and temperatures higher

than those experienced by the meteorite, for which Hollister et al. (2014) proposed pressures somewhat greater than 5 GPa and temperatures around 1200 °C.

The results of this study can be summarized as follows, 1) synthetic icosahedrite was shown to retain its structure up to ~50 GPa at ambient temperature; 2) it was experimentally demonstrated for the first time that pressure can stabilize the icosahedral AlCuFe quasicrystal until it melts (or decomposes) with no evidence of direct structural change to a crystalline phases; 3) congruent melting of icosahedrite might be limited to a very narrow temperature interval at 21 GPa and 1673 beyond which Al, Cu-rich phases would form. Based on our results the preservation of icosahedrite over cosmic time scales in a meteorite that formed at the early stage of the solar system results from its unexpected stability at high temperatures and pressures. Therefore, the discovery of icosahedrite in other meteorites exposed to extreme conditions and with bulk compositions similar Khatyrka should be expected.

Acknowledgments

This work was partially supported by EFree, an Energy Frontier Research Center funded by the US DOE, Office of Science, Basic Energy funded under award DE-SC-000157 and by CDAC under US DOE/NNSA award DE-NA-0006. Part of this work was performed at GeoSoilEnviroCARS (Sector 13), Advanced Photon Source (APS), Argonne National Laboratory (ANL). GeoSoilEnviroCARS is supported by the National Science Foundation award EAR-1128799 and DOE award DEFG02-94ER14466. Part of this work was also performed at HPCAT (Sector 16), Advanced Photon Source (APS), Argonne National Laboratory. HPCAT operations are supported by DOE/NNSA under award DE-NA0001974 and DOE-BES

340 award DE-FG02-99ER45775, with partial instrumentation funding by NSF. The Advanced
341 Photon Source is a DOE Office of Science User Facility operated for the DOE Office of Science
342 by ANL under Contract DE-AC02-06CH11357.

343

344 **References**

345 Angel, R.J., Bujak, M., Zhao, J., Gatta, G.D., and Jacobsen, S.D. (2007) Effective hydrostatic
346 limits of pressure media for high-pressure crystallographic studies. Journal of Applied
347 Crystallography, 40, 26.
348 Angel, R.J., Gonzalez-Platas, J., and Alvaro, M. (2014) EosFit7c and a Fortran module (library)
349 for equation of state calculations. Zeitschrift für Kristallographie, 229, 405–419.
350 Bancel, P.A. (1999) Order and disorder in icosahedral alloys. Quasicrystals. In DiVincenzo D.P.
351 and Steinhardt P.J., Eds, Series on Directions in Condensed Matter Physics, World
352 Scientific, 16, 17–55.
353 Bindi, L., Steinhardt, P.J., Yao, N., and Lu, P.J. (2009) Natural Quasicrystals. Science, 324,
354 1306–1309.
355 Bindi, L., Steinhardt, P.J., Yao, N., and Lu, P.J. (2011) Icosahedrite, $Al_{63}Cu_{24}Fe_{13}$, the first
356 natural quasicrystal. American Mineralogist, 96, 928–931.
357 Bindi, L., Eiler, J.M., Guan, Y., Hollister, L.S., MacPherson, G., Steinhardt, P.J., and Yao, N.
358 (2012) Evidence for the extraterrestrial origin of a natural quasicrystal. Proceedings of the
359 National Academy of Sciences, 109, 1396–1401.
360 Dewaele, A., Loubeyre, P., and Mezouar, M. (2004) Equations of state of six metals above 94
361 GPa. Physical Review B, 70(9), 094112.

Hammersley, A.P., (1998) FIT2D V12.077 Reference Manual, European Synchrotron Radiation Facility, Grenoble, France, Version 4.0.

Hemley, R.J., Zha, C.S., Jephcoat, A.P., Mao, H.-K., Finger, L.W., and Cox, D.E. (1989) X-ray diffraction and equation of state of solid neon to 110 GPa. Physical Review B, 39(16), 11820–11827.

Hirose, K. and Fei, Y. (2002) Subsolidus and melting phase relations of basaltic composition in the uppermost lower mantle. Geochimica et Cosmochimica Acta, 66, 2099–2108.

Hollister, L.S., Bindi, L., Yao, N., Poirier, G.R., Andronicos, C.L., MacPherson, G.J., Lin, C., Distler, V.V., Eddy, M.P., Kostin, A., Kryachko, V., Steinhardt, W.M., Yudovskaya, M., Eiler, J.M., Guan, Y., Clarke, J.J., and Steinhardt, P.J. (2014) Impact-induced shock and the formation of natural quasicrystals in the early solar system. Nature Communications, 5, 1–8.

Itie, J.P., Lefebvre, S., Sadoc, A., Capitan, M.J., Bessiere, M., Calvayrac, Y., and Polian, A. (1996) X-ray absorption and diffraction study of the stability of two quasicrystals (AlCuFe and AlCuLi) under high pressure. In C. Janot, and R. Mosseri, Eds., Proceedings of the Fifth International Conference on Quasicrystals, pp. 168. Singapore: World Scientific.

Janot, C. (1994) Quasicrystals: A Primer. Oxford University Press, Oxford.

Lefebvre, S., Bessiére, M., Calvayrac, Y., Itie, J.P., Polian, A., and Sadoc, A. (1995) Stability of icosahedral Al-Cu-Fe and two approximant phases under high pressure up to 35 GPa. Philosophical Magazine B, 72, 101–113.

Levine, D., and Steinhardt, P.J. (1984) Quasicrystals: A new class of ordered structures. Physical Review Letters, 53, 2477–2480.

Lu, P.J., Deffeyes, K., Steinhardt, P.J., and Yao, N. (2001) Identifying and indexing icosahedral quasicrystals from powder diffraction patterns. Physical Review Letters, 87, 275507.

MacPherson, G.J., Andronicos, C.L., Bindi, L., Distler, V.V., Eddy, M.P., Eiler, J.M., Guan, Y., Hollister, L.S., Kostin, A., Kryachko, V., Steinhardt, W.M., Yudovskaya, M., and Steinhardt, P.J. (2013) Khatyrka, a new CV3 find from the Koryak Mountains, Eastern Russia. Meteoritics and Planetary Science, 48, 1499–1514.

Mao, H.-K., Xu, J., and Bell, P.M. (1986) Calibration of the ruby pressure gauge to 800 kbar under quasi-hydrostatic conditions. Journal of Geophysical Research, 91(B5), 4673–4676.

Mao, H.-K., Wu, Y., Chen, L.C., Shu, J.F., and Jephcoat, A.P. (1990) Static compression of iron to 300 GPa and $Fe_{0.8}Ni_{0.2}$ alloy to 260 GPa: Implications for composition of the core. Journal of Geophysical Research, 95(B13), 21737–21742.

Prakapenka, V.B., Kubo, A., Kuznetsov, A., Laskin, A., Shkurikhin, O., Dera, P., Rivers, M.L., and Sutton, S.R. (2008) Advanced flat top laser heating system for high pressure research at GSECARS: application to the melting behavior of germanium. High Pressure Research, 28, 225–235.

Sadoc, A., Itie, J.P., Polian, A., Lefevbre, S., Bessiére, M., and Calvayrac, Y. (1994) X-ray absorption and diffraction spectroscopy of icosahedral Al-Cu-Fe quasicrystals under high pressure. Philosophical Magazine B, 70, 855–866.

Sadoc, A., Itie, J.P., Polian, A., Lefevbre, S., and Bessiére, M. (1995) Quasicrystals under high pressure. Physica B, 208-209, 495–496.

Shechtman, D., Blech, I., Gratias, D., and Cahn, J. (1984) Metallic phase with long-range orientational order and no translational symmetry. Physical Review Letter, 53, 1951–1954.

406 Stagno, V., Bindi, L., Shibazaki, Y., Tange, Y., Higo, Y., Mao, H.-K., Steinhardt, P.J., and Fei,
407 Y. (2014) Icosahedral AlCuFe quasicrystal at high pressure and temperature and its
408 implications for the stability of icosahedrite. Scientific Reports, 4, 5869.
409 Steurer, W., and Deloudi, S. (2009) Crystallography of Quasicrystals. Concepts, Methods and
410 Structures. Springer, Berlin.
411 Tsai, A.P. (2013) Discovery of stable icosahedral quasicrystals: progress in understanding
412 structure and properties. Chemical Society Reviews, 42, 5352–5365.
413 Zhang, L., and Lück, R. (2003a) Phase diagram of the Al-Cu-Fe quasicrystal-forming alloy
414 system. I. Liquidus surface and phase equilibria with liquid. Zeitschrift für Metallkunde,
415 94, 91–97.
416 Zhang, L., and Lück, R. (2003b) Phase diagram of the Al–Cu–Fe quasicrystal-forming alloy
417 system. II. Liquidus surface and phase equilibria with liquid. Zeitschrift für Metallkunde,
418 94, 98–107.
419 Zhang, L., and Lück, R. (2003c) Phase diagram of the Al–Cu–Fe quasicrystal-forming alloy
420 system. III. Liquidus surface and phase equilibria with liquid. Zeitschrift für Metallkunde,
421 94, 108–115.
422 Zhang, L., and Lück, R. (2003d) Phase diagram of the Al–Cu–Fe quasicrystal-forming alloy
423 system. IV. Liquidus surface and phase equilibria with liquid. Zeitschrift für Metallkunde,
424 94, 341–344.
425 Zhang, L., and Lück, R. (2003e) Phase diagram of the Al-Cu-Fe quasicrystal-forming alloy
426 system. V. Solidification behavior of Al-Cu-Fe quasicrystal forming alloys. Zeitschrift für
427 Metallkunde, 94, 774–781.
428

Figure Captions

Figure 1. Representative X-ray diffraction pattern of i-$Al_{63}Cu_{24}Fe_{13}$ collected at P = 18.5 GPa. Diffraction rings and weak single spots are typical features of the collected patterns. The Debye-Scherrer rings are labeled as in case of QCs using the two-integer indexes by Janot (1994). The diffraction patterns were processed using Fit2D (Hammersley 1998) and Peakfit software.

Figure 2. Pressure dependence of the powder X-ray diffraction patterns of i-QC collected at room temperature in angle-dispersive mode (wavelength of 0.4246 Å). Filled circles indicate peaks of ruby (pressure marker), grey circles for Au (pressure marker), empty circles for Re (gasket) filled triangles for Ne (pressure medium). The diffraction peaks were indexed using Cahn indices (N, M) following the scheme proposed by Janot (1994; see also Steurer and Deloudi 2009). The diffraction pattern (in gray) at ambient pressure is relative to the sample after decompression.

Figure 3. Variation of the lattice parameter as function of pressure: yellow square, ambient pressure value (Bindi et al. 2011); black and white squares indicate lattice parameter determined respectively from compression and decompression experiments; gray squares indicate experiments at higher resolution.

Figure 4. Pressure-volume relations for i-$Al_{64}Cu_{23}Fe_{13}$ with experimental data (black squares) fitted using a Murnaghan EOS (dashed black line). Results from Birch-Murnaghan and Vinet et al. EOS fits are here omitted since both closely overlap the Murnaghan EOS fit. Uncertainties are within the symbol size. Our fit is compared with previous studies by Sadoc et al. (1994; gray

line) and Lefbvre et al. (1995; blue line) both for icosahedral $Al_{62}Cu_{25.5}Fe_{12.5}$ and for one approximant phase with composition $Al_{64}Cu_{24}Fe_{12}$ (Lefbvre et al. 1995; yellow line). The two curves obtained from these previous studies are extrapolated up to 52 GPa assuming that no structural phase transformation occurs. The EOS of pure Al, Cu (Dewaele et al. 2004) and Fe (Mao et al. 1990) are also reported with green, blue and brown, respectively.

Figure 5. Representative angle-dispersive (wavelength of 0.4133 Å) X-ray diffraction patterns for synthetic icosahedrite as function of temperature at ~ 42 GPa. Diffraction patterns were collected with 15s exposure time after keeping the sample at approximately constant *T* for 180s. Peaks are indexed as mentioned above. Filled black triangles indicate the (111) and (200) peaks of Ne pressure medium. The figure demonstrates the stability of i-QC during heating up to about 1830 K followed by slow cooling down to 1000 K before quench.

Figure 6. Back-scattered electron (BSE) images of the recovered sample from runs at 21 GPa. a) Run at 1673 K showing the presence of i-QC also confirmed by the five-fold symmetry in (b) using single crystal X-ray diffraction. (c) Recovered sample from 21 GPa and 1773 K and d) 1973 K, respectively.

Figures

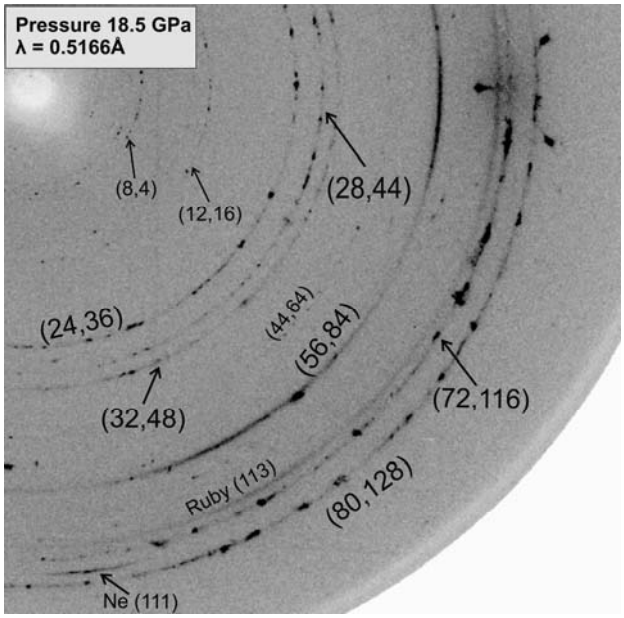

Figure 1

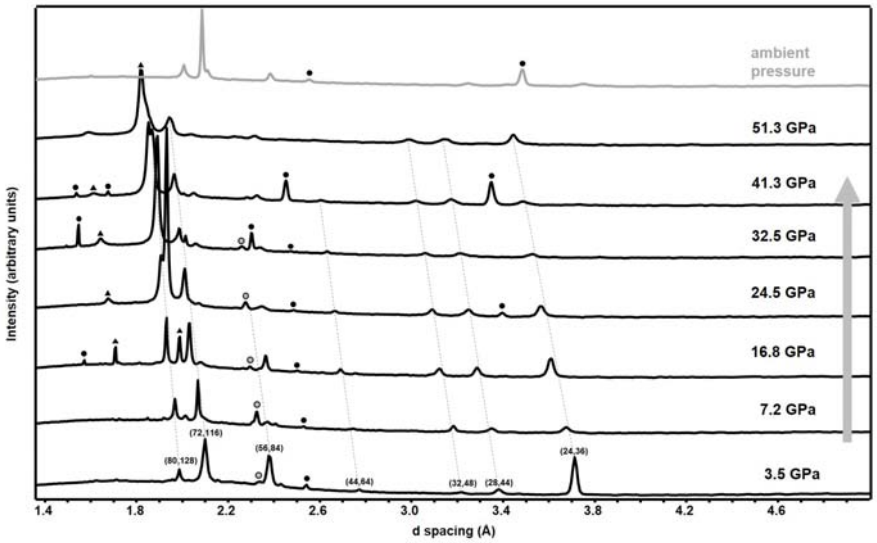

Figure 2

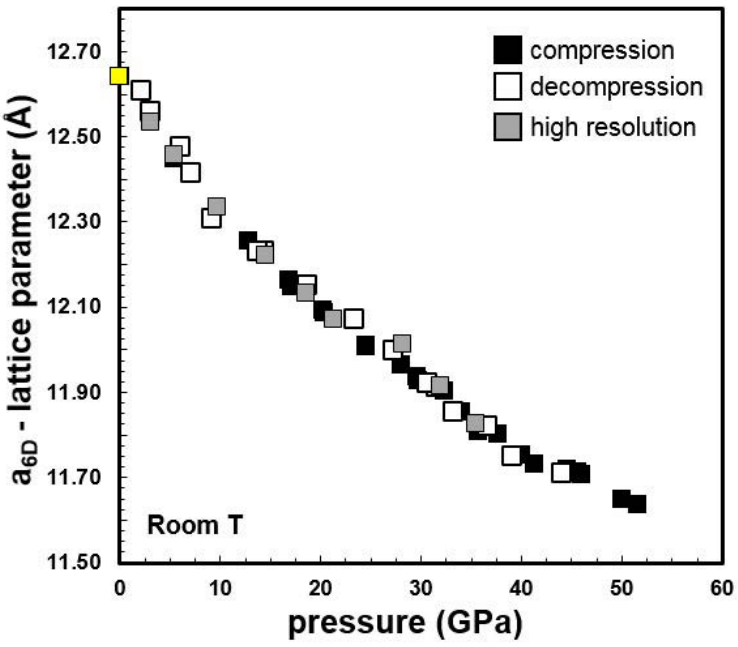

481

482 Figure 3

483

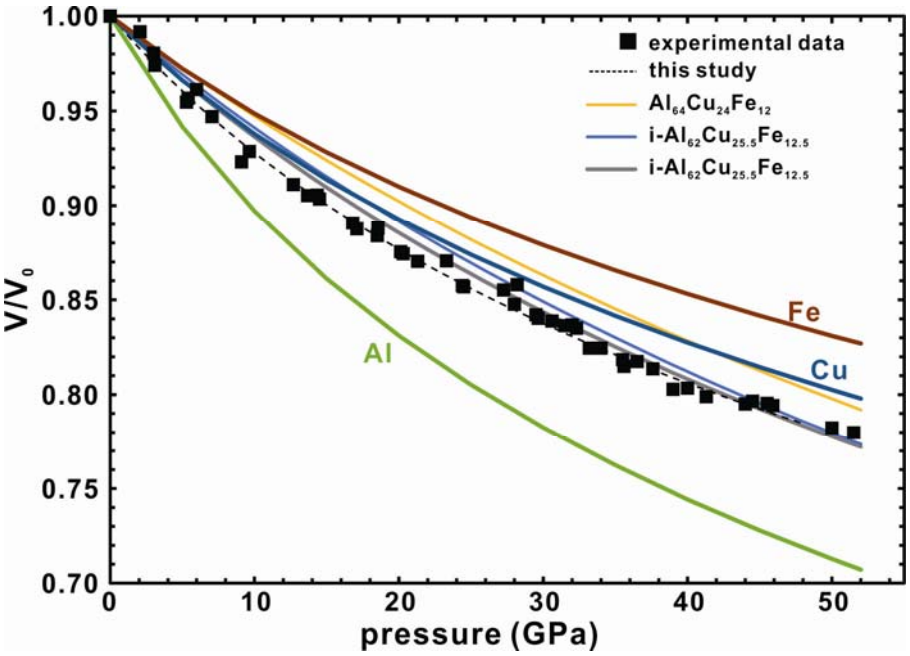

484

485 Figure 4

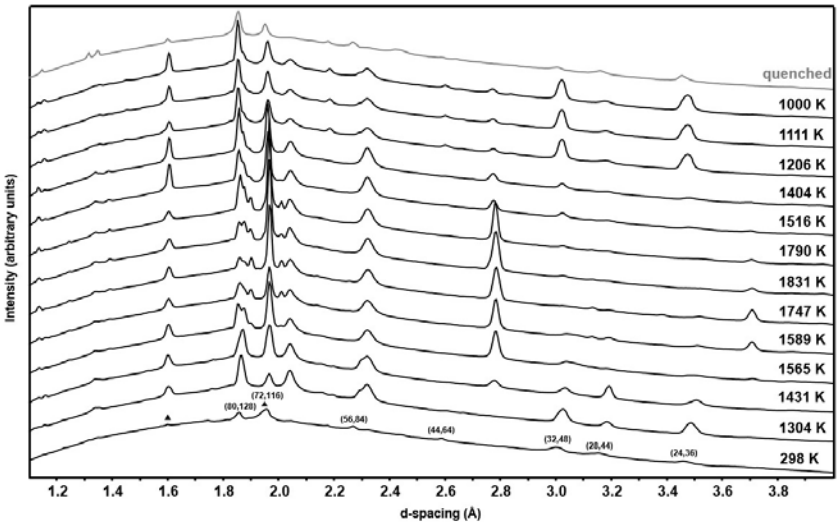

Figure 5

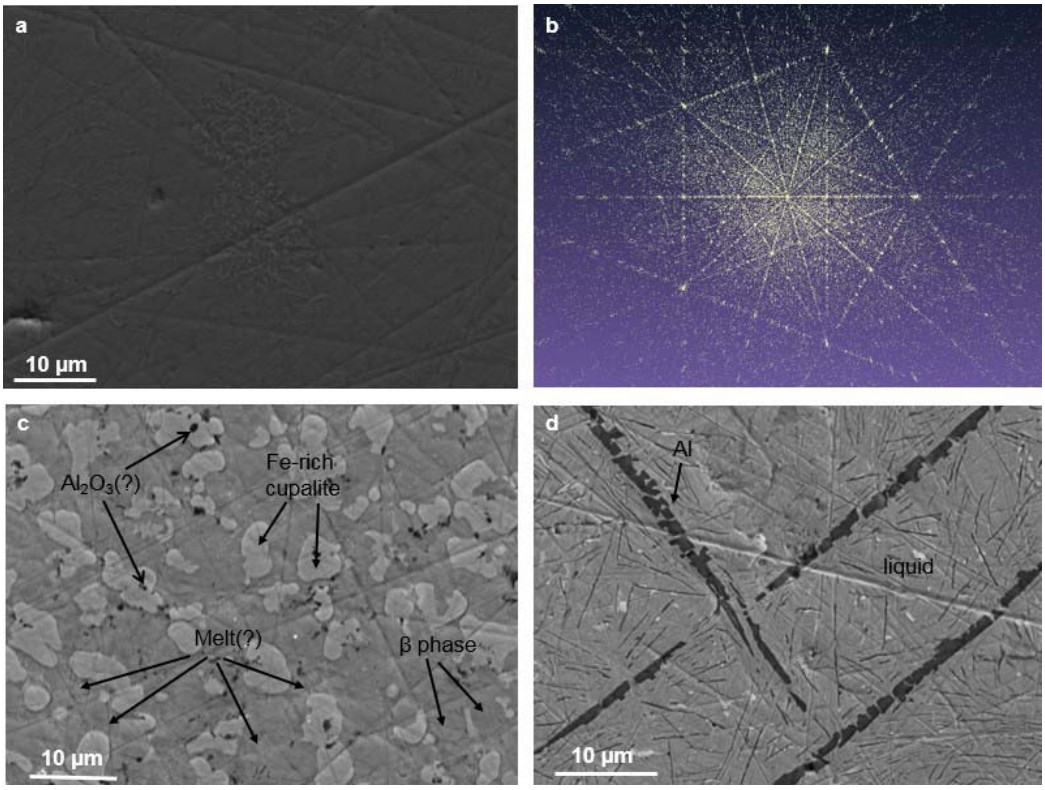

Figure 6